Microwave Spectrum of Butyronitrile: Methyl Internal Rotation and ^{14}N Quadrupole Coupling

Kirsten Vormann and Helmut Dreizler

Abteilung Chemische Physik im Institut für Physikalische Chemie der Universität Kiel

Z. Naturforsch. **43a**, 338–344 (1988); received February 6, 1988

We determined the internal rotation parameters of butyronitrile, antiperiplanar and synclinal, in the internal rotation ground state. The ^{14}N quadrupole coupling constants were refined.

The microwave spectrum of butyronitrile (n-propyl nitrile), $CH_3CH_2CH_2CN$, was first investigated by Hirota [1] who assigned μ_a and μ_b transitions of the type $J_{1K-1} - J_{0K}$ of the antiperiplanar (trans) form and μ_a and μ_b transitions of the synclinal (gauche) form. Later Kaushik [2] performed a centrifugal distortion analysis for the synclinal form based on the measurements of [1]. The ^{14}N quadrupole hyperfine structure (hfs) was analysed by Demaison and Dreizler [3] using microwave Fourier transform (MWFT) spectroscopy. The molecule was also the object of a low resolution study [4].

We present an investigation of the methyl internal rotation and a refinement of the quadrupole coupling constants. The internal rotation fine structure is quite narrow, therefore it could not be resolved by Stark spectroscopy. A centrifugal distortion analysis was necessary to confirm the assignment of high J transitions, which showed internal rotation splittings. Simultaneously Wlodarczak et al. [5] investigated the centrifugal distortion including the millimeter wave spectrum and measured the dipole moment and the energy difference between both conformers.

Butyronitrile was obtained from Fa. Merck, Darmstadt and used without further purification. The spectra were recorded with our MWFT spectrometers [6–8] in the range from 4.8 to 26.4 GHz, temperatures between -30° and -50 °C and pressures between 0.013–0.065 Pa (0.1 and 0.5 mTorr).

The prediction of higher J lines was impossible for the antiperiplanar form, using the transition frequencies given in [1]. Therefore we performed a double resonance experiment with the MWFT technique [9]. The pump transition $J_{K-K+} = 16_{1\,15} - 16_{0\,16}$ and a signal transition $J_{K-K+} = 16_{1\,15} - 15_{2\,14}$ were selected. With this information the assignment of the high J lines was possible. For the synclinal form the transitions reported in [1] were sufficient for a prediction of high J lines. A part of the measured transitions is given in Tables 1 and 2. A complete list has been deposited under number TNA 15 at the library of the University of Kiel, Universitätsbibliothek, Westring 400, D-2300 Kiel. All frequencies were determined by a least squares fit of the time domain signals of the multiplets to minimize overlapping effects [10, 11]. In Fig. 1 and 2 we present typical recordings in the form of power spectra. The assignment of the transitions was confirmed by a centrifugal distortion analysis and by the consistency of the hfs and internal rotation analysis. The Watson A reduction [12] of fourth order was used for the antiperiplanar form. For the synclinal form the corresponding reduction of sixth order was used, including the transitions given in [5]. For these analyses the hypothetical unsplit lines with frequency ν_0 were used, which were calculated by adding the hfs and internal rotation splittings to the multiplet components. The results of the centrifugal distortion analyses are given in Tables 3 and 4. In the analysis of the nuclear quadrupole hyperfine structure and the internal rotation it was assumed that both perturbations of the spectrum are independent from each other. The A and E internal rotation components show equal hfs multiplets.

An analysis of first order [13] was sufficient for the hfs. The results are given in Tables 5 and 6. The accuracy could be increased at least by a factor of five in comparison to [3].

The internal rotation splittings were analysed by IAM in the formulation of Woods [14–16]. Only the internal rotation splittings of the most intensive qua-

Reprint requests to Prof. Dr. H. Dreizler, Institut für Physikalische Chemie der Universität Kiel, Olshausenstr. 40–60, D-2300 Kiel.

0932-0784 / 88 / 0400-0338 $ 01.30/0. – Please order a reprint rather than making your own copy.

Table 1. Measured transitions of antiperiplanar butyronitrile. Γ: Symmetry species, ν: experimental frequency, $\Delta\nu_{hfs}$: measured A-species ^{14}N hfs shift related to the most intensive component, $\Delta\nu_{AE}$: experimental torsional splitting, ν_0: centre frequency, δ_{hfs}: difference between calculated and experimental hfs splitting, δ: difference between calculated and experimental torsional splitting, δ_0: difference between calculated and experimental centre frequency, *: used for the hfs analysis.

J	K_-	$K_+ - J'$	K'_-	K'_+	$F - F'$	Γ	ν [MHz]	$\Delta\nu_{hfs}$ [MHz]	δ_{hfs} [MHz]	$\Delta\nu_{AE}$ [MHz]	δ [MHz]	ν_0 [MHz]	δ_0 [MHz]
3	0	3 – 2	0	2	4 – 3	A	13 261.477					13 261.436	−0.010
		*						0.044	0.001				
					3 – 2	A	13 261.433						
								0.215	−0.002				
					2 – 1	A	13 261.262						
3	2	2 – 2	2	1	4 – 3	A	13 263.790						
					4 – 3	E	13 263.991			−0.201	0.006	13 263.547	−0.005
								1.106	0.001				
					3 – 2	A	13 262.685						
4	2	3 – 3	2	2	5 – 4	A	17 684.440						
					5 – 4	E	17 684.501			−0.061	0.004	17 684.317	0.001
								0.467	0.002				
					4 – 3	A	17 683.973						
					4 – 3	E	17 684.037			−0.064	0.007		
								−0.123	0.002				
					3 – 2	A	17 684.563						
					3 – 2	E	17 684.622			−0.059	0.002		
5	3	2 – 4	3	1	6 – 5	A	22 108.066					22 107.924	0.004
		*						0.530	−0.001				
					5 – 4	A	22 107.536						
								−0.127	0.003				
					4 – 3	A	22 108.193						
9	1	8 – 9	0	9	10 – 10	A	24 166.222						
					8 – 8	E	24 166.160			0.062	0.000	24 166.242	−0.010
		*						−0.181	0.000				
					9 – 9	A	24 166.403						
					9 – 9	E	24 166.343			0.060	0.002		
16	1	15 – 15	2	14	17 – 16	A	13 991.954						
					15 – 14	E	13 992.124			−0.170	0.002	13 992.090	−0.037
								−0.073	0.003				
					16 – 15	A	13 992.027						
					16 – 15	E	13 992.195			−0.168	0.000		
17	1	16 – 16	2	15	18 – 17	A	19 339.325						
					16 – 15	E	19 339.492			−0.166	−0.001	19 339.460	−0.033
		*						−0.077	0.002				
					17 – 16	A	19 339.402						
					17 – 16	E	19 339.569			−0.167	0.000		
17	3	15 – 18	2	16		A	26 095.257						
						E	26 094.969			0.288	−0.003	26 095.072	0.026
18	3	16 – 19	2	17		A	21 310.238						
						E	21 309.953			0.285	−0.003	21 310.053	0.023
19	1	19 – 18	2	16	20 – 19	A	6 197.030						
					18 – 17	E	6 197.208			−0.178	0.001	6 197.075	0.000
								0.222	−0.002				
					19 – 18	A	6 196.808			−0.183	0.006		
					19 – 18	E	6 196.991						
19	3	16 – 20	2	19	20 – 21	A	19 831.485						
					18 – 19	E	19 831.217			0.268	0.004	19 831.330	0.019
								−0.071	0.004				
					19 – 20	A	19 831.556						
					19 – 20	E	19 831.291			0.265	0.007		
20	3	18 – 21	2	19		A	11 570.165						
						E	11 569.885			0.280	−0.004	11 569.979	0.019
21	3	19 – 22	2	20		A	6 607.517			0.279	−0.002	6 607.331	0.014
						E	6 607.238						
22	3	19 – 23	2	22	23 – 24	A	7 318.691						
					21 – 22	E	7 318.421			0.270	−0.001	7 318.534	0.019
								−0.065	0.004				
					22 – 23	A	7 318.756						
					22 – 23	E	7 318.486			0.270	−0.001		

Table 1 (continued)

J	K_-	$K_+ - J'$	K'_-	K'_+	$F - F'$	Γ	ν [MHz]	$\Delta\nu_{hfs}$ [MHz]	δ_{hfs} [MHz]	$\Delta\nu_{AE}$ [MHz]	δ [MHz]	ν_0 [MHz]	δ_0 [MHz]
28	2	26 – 27	3	25	29 – 28	A	24 644.554						
					27 – 26	E	24 644.834				−0.280	0.002	24 644.757	0.046
								−0.054	0.005				
					28 – 27	A	24 644.608						
					28 – 27	E	24 644.891				−0.283	0.005		
27	4	23 – 28	3	26		A	26 014.590						
						E	26 014.280				0.310	0.007	26 014.363	−0.003
28	2	27 – 27	3	24	29 – 28	A	12 629.694						
					27 – 26	E	12 629.961				−0.267	0.003	12 629.848	−0.009
								0.070	0.000				
					28 – 27	A	12 629.624						
					28 – 27	E	12 629.893				−0.269	0.005		
28	4	25 – 29	3	26		A	20 524.108						
						E	20 523.737				0.371	0.001	20 523.876	−0.023
28	4	24 – 29	3	27		A	21 572.813						
						E	21 572.488				0.325	−0.001	21 572.582	−0.001
29	2	28 – 28	3	25	30 – 29	A	16 441.424						
					28 – 27	E	16 441.682				−0.258	−0.004	16 441.572	0.000
								0.075	−0.003				
					29 – 28	A	16 441.349						
					29 – 28	E	16 441.605				−0.256	−0.006		
30	2	29 – 29	3	26	31 – 30	A	20 181.403						
					29 – 28	E	20 181.664				−0.261	0.000	20 181.553	0.005
								0.074	−0.001				
					30 – 29	A	20 181.329						
					30 – 29	E	20 181.593				−0.264	0.003		
30	4	27 – 31	3	28		A	11 156.016						
						E	11 155.654				0.362	0.000	11 155.783	−0.019
31	2	30 – 30	3	27	32 – 31	A	23 843.792						
					30 – 29	E	23 844.052				−0.260	0.001	23 843.940	0.010
								0.079	−0.003				
					31 – 30	A	23 843.713						
					31 – 30	E	23 843.973				−0.260	0.001		
31	4	28 – 32	3	29		A	6 417.960						
						E	6 417.598				0.362	−0.002	6 417.726	−0.019
31	4	27 – 32	3	30		A	8 280.810						
						E	8 280.476				0.334	0.000	8 280.581	−0.010
36	3	33 – 35	4	32		A	12 979.388						
						E	12 979.744				−0.356	0.005	12 979.624	−0.012
36	3	34 – 35	4	31		A	9 299.566						
						E	9 299.902				−0.336	0.009	9 299.790	0.005
37	3	35 – 37	4	32		A	13 654.844						
						E	13 655.178				−0.334	−0.004	13 655.067	0.006
38	3	35 – 37	4	34		A	22 999.735						
						E	23 000.093				−0.358	0.006	22 999.972	−0.044
37	5	32 – 38	4	35		A	24 129.299						
						E	24 129.009				0.290	0.003	24 129.041	−0.016
38	5	34 – 39	4	35		A	19 274.897						
						E	19 274.435				0.462	0.002	19 274.638	0.018
39	5	34 – 40	4	37		A	15 111.089						
						E	15 110.764				0.325	0.006	15 110.833	0.028

Table 2. Measured transitions of synclinal butyronitrile. Γ: Symmetry species, ν: experimental frequency, $\Delta\nu_{\mathrm{hfs}}$: measured A-species ^{14}N hfs shift related to the most intensive component, $\Delta\nu_{\mathrm{AE}}$, $\Delta\nu_{\mathrm{AE}^*}$: experimental torsional splitting, ν_0: centre frequency, δ_{hfs}: difference between calculated and experimental hfs splitting, δ: difference between calculated and experimental torsional splitting, δ_0: difference between calculated and experimental centre frequency, *: used for the hfs analysis.

J	K_-	K_+	$-J'$	K'_-	K'_+	$F-F'$	Γ	ν [MHz]	$\Delta\nu_{\mathrm{hfs}}$ [MHz]	δ_{hfs} [MHz]	$\Delta\nu_{\mathrm{AE}}$ $\Delta\nu_{\mathrm{AE}^*}$ [MHz]	δ [MHz]	ν_0 [MHz]	δ_0 [MHz]
2	2	1	2	1	2	3 – 3	A	22 064.003					22 064.261	0.003
		*							−1.159	−0.003				
						2 – 2	A	22 065.162						
									0.650	−0.004				
						1 – 1	A	22 063.353						
3	1	3	2	1	2	4 – 3	A	17 055.670					17 055.610	−0.004
		*							0.173	−0.002				
						3 – 2	A	17 055.497						
									0.074	−0.006				
						2 – 1	A	17 055.596						
4	1	3	4	0	4	5 – 5	A	10 286.452					10 286.601	0.012
		*							−0.557	−0.001				
						4 – 4	A	10 287.009						
									0.142	0.001				
						3 – 3	A	10 286.310						
7	1	6	7	0	7	8 – 8	A	17 634.638					17 634.822	0.038
		*							−0.630	−0.001				
						7 – 7	A	17 635.268						
									0.090	0.001				
						6 – 6	A	17 634.548						
11	3	9	10	4	6	12 – 11	A	16 546.876					16 546.819	0.003
		*				10 – 9	A							
									0.170	0.000				
						11 – 10	A	16 546.706						
12	7	6	13	6	7	13 – 14	A	13 549.629						
						11 – 12	E	13 549.567			0.062	0.003	13 549.701	0.001
							E*	13 550.948			−1.319	0.004		
									−0.206	0.003				
						12 – 13	A	13 549.835						
12	7	5	13	6	8	13 – 14	A	13 551.026						
						11 – 12	E	13 551.100			−0.074	0.001	13 551.095	−0.004
							E*	13 549.716			1.310	−0.002		
									−0.203	0.000				
						12 – 13	A	13 551.229						
						12 – 13	E	13 551.306			−0.077	0.004		
13	7	7	14	6	8	14 – 15	A	7 398.340						
						12 – 13	E	7 398.293			0.047	0.008	7 398.401	0.001
							E*	7 401.707			−3.367	0.002		
									−0.159	−0.006				
						13 – 14	A	7 398.499						
						13 – 14	E	7 398.443			0.056	−0.001		
13	7	6	14	6	9	14 – 15	A	7 401.794						
						12 – 13	E	7 401.864			−0.070	0.006	7 401.855	−0.005
							E*	7 398.443			3.351	0.006		
									−0.167	0.002				
						13 – 14	A	7 401.961						
						13 – 14	E	7 402.038			−0.077	0.013		
15	8	8	16	7	9	16 – 17	A	9 498.185						
						14 – 15	E	9 498.103			0.082	0.001	9 498.238	0.005
							E*	9 498.675			−0.490	0.002		
									−0.156	0.009				
						15 – 16	A	9 498.341						
						15 – 16	E	9 498.270			0.073	0.010		
							E*	9 498.829			−0.488	0.000		
15	8	7	16	7	10	16 – 17	A	9 498.738						
						14 – 15	E	9 498.829			−0.091	0.000	9 498.794	0.006
							E*	9 498.270			0.468	0.011		
									−0.152	0.005				
						15 – 16	A	9 498.890						
						15 – 16	E	9 498.971			−0.081	0.010		

Table 2 (continued)

J	K_-	K_+	$-J'$	K'_-	K'_+	$F-F'$	Γ	ν [MHz]	$\Delta\nu_{\mathrm{hfs}}$ [MHz]	δ_{hfs} [MHz]	$\Delta\nu_{\mathrm{AE}}$ $\Delta\nu_{\mathrm{AE}^*}$ [MHz]	δ [MHz]	ν_0 [MHz]	δ_0 [MHz]
19	7	12	18	8	11	20 – 19	A	9 123.220						
						18 – 17	E	9 123.261			−0.041	0.003	9 123.186	0.006
							E*	9 116.942			6.278	0.000		
									0.089	0.000				
						19 – 18	A	9 116.131						
						19 – 18	E	9 116.088			−0.043	0.005		
19	7	12	18	8	11	20 – 19	A	9 116.815						
						18 – 17	E	9 116.763			0.052	−0.001	9 116.781	0.006
							E*	9 123.084			−6.269	0.004		
									0.092	−0.004				
						19 – 18	A	9 116.723						
						19 – 18	E	9 116.674			0.049	0.003		
22	8	14	21	9	13	23 – 22	A	13 221.121						
						21 – 20	E	13 221.182			−0.061	0.001	13 221.090	0.005
							E*	13 218.913			2.208	−0.005		
									0.071	−0.003				
						22 – 21	A	13 221.050						
						22 – 21	E	13 221.121			−0.071	0.011		
22	8	15	21	9	12	23 – 22	A	13 218.822						
						21 – 20	E	13 218.748			0.074	0.000	13 218.792	0.007
							E*	13 221.008			−2.186	−0.002		
									0.074	0.000				
						22 – 21	A	13 218.748						
						22 – 21	E	13 218.678			0.070	+0.004		
						22 – 21	E*	13 220.935			−2.187	−0.001		
22	4	18	22	4	19	23 – 23	A	25 543.625						
						21 – 21	E	25 543.591			0.034	−0.001	25 543.715	0.029
									−0.335	−0.004				
						22 – 22	A	25 543.960						
						22 – 22	E	25 543.929			0.031	0.002		
23	8	15	22	9	14	24 – 23	A	19 511.234						
						22 – 21	E	19 511.278			−0.044	0.002	19 511.211	0.006
							E*	19 506.683			4.551	0.009		
									0.060	0.003				
						23 – 22	A	19 511.174						
23	8	16	22	9	13	24 – 23	A	19 506.557						
						22 – 21	E	19 506.489			0.068	−0.010	19 506.528	0.008
							E*	19 511.103			−4.546	0.002		
									0.068	−0.005				
						23 – 22	A	19 506.489						
24	3	21	25	2	24	25 – 26	A	5 073.792						
						23 – 24	E	5 073.724			0.068	0.005	5 073.952	−0.002
									−0.614	−0.001				
						24 – 25	A	5 074.406						
						24 – 25	E	5 074.337			0.069	0.006		
25	5	20	25	5	21	26 – 26	A	16 254.900						
						24 – 24	E	16 254.865			0.035	−0.005	16 254.957	−0.009
									−0.241	0.003				
						25 – 25	A	16 255.141						
						25 – 25	E	16 255.104			0.037	0.007		
26	5	21	26	5	22	27 – 27	A	21 090.027						
						25 – 25	E	21 089.987			0.040	−0.005	21 090.090	−0.016
									−0.265	0.002				
						26 – 26	A	21 090.292						
						26 – 26	E	21 090.252			0.040	−0.005		
28	3	26	27	4	23	29 – 28	A	19 892.073						
						27 – 26	E	19 892.146			−0.073	−0.002	19 891.926	0.069
									0.590	−0.003				
						28 – 27	A	19 891.483						
						28 – 27	E	19 891.559			−0.076	−0.001		
30	6	24	30	6	25	31 – 31	A	16 246.345						
						29 – 29	E	16 246.309			0.036	−0.002	16 246.388	−0.049
									−0.202	0.001				
						30 – 30	A	16 246.547						
						30 – 30	E	16 246.510			0.037	−0.003		
34	7	27	34	7	28	35 – 35	A	11 727.754						
						33 – 33	E	11 727.723			0.031	−0.001	11 727.780	−0.050
									−0.142	0.000				
						34 – 34	A	11 727.896						
						34 – 34	E	11 727.864			0.032	−0.002		

Table 2 (continued)

J	K_-	K_+	$-J'$	K'_-	K'_+	$F-F'$	Γ	ν [MHz]	$\Delta\nu_{hfs}$ [MHz]	δ_{hfs} [MHz]	$\Delta\nu_{AE}$ $\Delta\nu_{AE}$ [MHz]	δ [MHz]	ν_0 [MHz]	δ_0 [MHz]
36	7	29	36	7	30	37 – 37	A	20 572.848						
						35 – 35	E	20 572.797	−0.197	0.001	0.051	−0.006	20 572.880	−0.040
						36 – 36	A	20 573.045						
						36 – 36	E	20 572.995			0.050	−0.005		
36	4	32	37	3	35	37 – 38	A	19 547.824						
						35 – 36	E	19 547.744	−0.372	−0.012	0.080	−0.002	19 547.899	−0.045
						36 – 37	A	19 458.196						
						36 – 37	E	19 458.117			0.079	0.000		
37	7	30	37	7	31	38 – 38	A	26 237.893						
						36 – 36	E	26 237.843	−0.226	0.004	0.050	0.003	26 237.933	−0.025
						37 – 37	E	26 238.119						
						37 – 37	E	26 238.066			0.053	0.000		
38	4	35	37	5	32	39 – 38	A	9 991.701						
						37 – 36	E	9 991.786	0.419	0.004	−0.085	−0.004	9 991.617	−0.007
						38 – 37	A	9 991.282						
						38 – 37	E	9 991.364			−0.082	−0.007		
39	4	36	38	5	33	40 – 39	A	5 311.296						
						38 – 37	E	5 311.377	0.402	−0.001	−0.081	−0.006	5 311.217	−0.069
						39 – 38	A	5 310.894						
						39 – 38	E	5 310.979			−0.085	−0.002		
39	8	31	39	8	32	40 – 40	A	11 013.019						
						38 – 38	E	11 012.989	−0.119	0.002	0.030	0.000	11 013.037	−0.003
						39 – 39	A	11 013.138						
						39 – 39	E	11 013.105			0.033	−0.003		

Table 3. Rotational and centrifugal distortion constants of antiperiplanar butyronitrile.

A	= 23668.320	(7) MHz	δ_J	= 0.04627	(14) kHz
B	= 2268.1467	(8) MHz	δ_K	= 0.835	(49) kHz
C	= 2152.9610	(7) MHz	æ	= −0.989293	
Δ_J	= 0.3952	(19) kHz	σ	= 21	kHz
Δ_{JK}	= −10.905	(56) kHz			
Δ_K	= 241.28	(66) kHz			

Correlation coefficient matrix:

A	1.000							
B	0.958	1.000						
C	0.961	0.973	1.000					
Δ_J	0.481	0.611	0.527	1.000				
Δ_{JK}	0.411	0.526	0.447	0.986	1.000			
Δ_K	−0.271	−0.391	−0.314	−0.941	−0.982	1.000		
δ_J	−0.011	−0.034	0.053	0.347	0.485	−0.566	1.000	
δ_K	0.170	0.278	0.191	0.106	−0.043	0.144	−0.841	1.000

Table 4. Rotational and centrifugal distortion constants of synclinal butyronitrile. Transitions given in [5] up to $J = 50$ are included in the fit. $|(\quad)|$ highest correlation coefficient.

A	= 10060.416	(3) MHz	Φ_J	= 0.00579	(16) Hz
B	= 3267.6793	(8) MHz	Φ_{JK}	= 0.0250	(48) Hz
C	= 2705.4433	(7) MHz	Φ_{KJ}	= −0.564	(17) Hz
Δ_J	= 3.34948	(52) kHz	Φ_K	= 1.80	(13) Hz
Δ_{JK}	= −19.1862	(18) kHz	ϕ_J	= 0.003088	(90) Hz
Δ_K	= 60.998	(34) kHz	ϕ_{JK}	= −0.0217	(49) Hz
δ_J	= 1.0386	(22) kHz	ϕ_K	= 0.380	(92) Hz
δ_K	= 7.779	(10) kHz	æ	= −0.847114	
			σ	= 52	kHz

$|(\Phi_{KJ}, \phi_K)| = 0.997$

Table 5. Quadrupole coupling constants of antiperiplanar butyronitrile. Standard deviation of the hfs analysis of 17 splittings is 2 kHz, mean splitting is 390 kHz.

	Correlation coefficient matrix	
$\chi^+(^{14}N)$ = 3.440 (4) MHz	1.000	
$\chi^-(^{14}N)$ = −0.671 (5) MHz	0.018	1.000
$\chi_{aa}(^{14}N)$ = −3.440 (4) MHz		
$\chi_{bb}(^{14}N)$ = 1.385 (5) MHz		
$\chi_{cc}(^{14}N)$ = 2.056 (5) MHz		

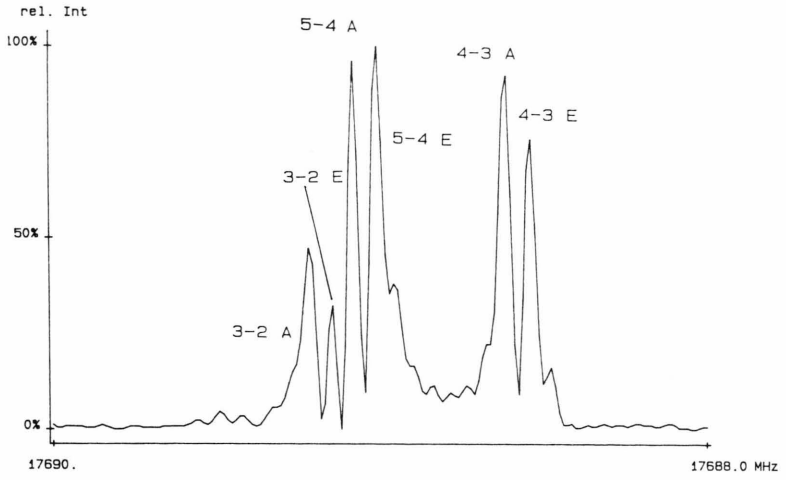

Fig. 1. $J_{K-K+} = 4_{22} - 3_{21}$ transition of antiperiplanar butyronitrile with internal rotation splittings and hfs hyperfine structure. The F quantum numbers and torsion A and E species are given in addition. Polarizing frequency 17 687.0 MHz. Sample interval 20 ns, 1024 sampling points. Zero filling to 4096 points prior to Fourier transformation, $6.6 \cdot 10^6$ averaging cycles, Temperature -50 °C, pressure 0.1 mTorr.

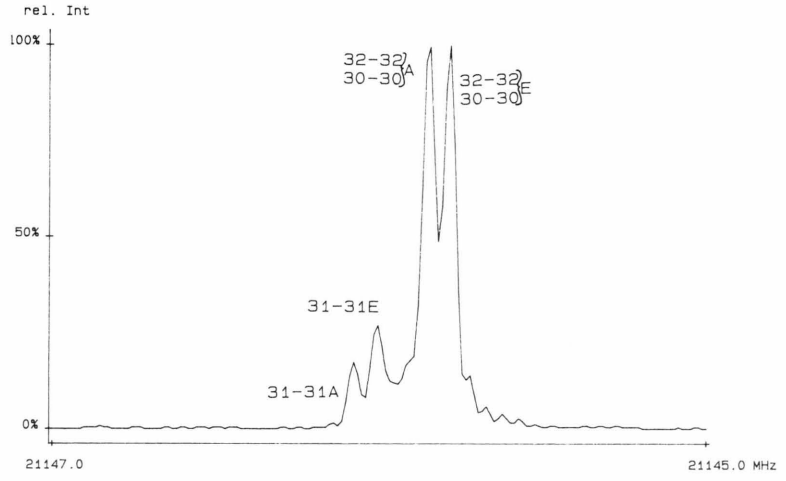

Fig. 2. $J_{K-K+} = 31_{6\,25} - 31_{6\,26}$ transition of synclinal butyronitrile with internal rotation splittings and hfs hyperfine structure. The F quantum numbers are given in addition. Polarizing frequency 21 146.5 MHz. Sample interval 50 ns, 1024 sampling points. Zero filling to 4096 points prior to Fourier transformation, $1.7 \cdot 10^7$ averaging cycles, Temperature -50 °C, pressure 0.3 mTorr.

Table 6. Quadrupole coupling constants of synclinal butyronitrile. Standard deviation of the hfs analysis of 20 splittings is 3 kHz, mean splitting is 302 kHz.

	Correlation coefficient matrix	
$\chi^+(^{14}N) = +1.683(4)$ MHz	1.000	
$\chi^-(^{14}N) = -2.186(5)$ MHz	0.162	1.000
$\chi_{aa}(^{14}N) = -1.683(4)$ MHz		
$\chi_{bb}(^{14}N) = -0.252(5)$ MHz		
$\chi_{cc}(^{14}N) = 1.935(5)$ MHz		

drupole components were used. For the antiperiplanar form the 45 measured splittings contained enough information to determine the reduced barrier s, the moment of inertia of the methyl group I_α, and the angle between the internal rotation axis and the inertia axis a. The results are given in Table 7.

The internal rotation axis of the synclinal form does not lie in a plane of the inertia axes. Two angles describe the position of the internal rotation axis with respect to the inertia axis. Although 37 transitions with A−E and partly with A−E* splittings were measured we had to assume I_α. The value of the antiperiplanar form was assumed for the synclinal form. The results are given in Table 8. To get the results of Tables 3 to 8 the complete list of lines has to be used.

In Table 9 we compare the internal rotation parameters of some propyl compounds in the torsional ground state. Propane, which is a molecule with two internal methyl rotors, possesses the highest barrier height V_3. The two rotational isomers of butyronitrile surprisingly have the same barrier height V_3 within the standard deviation. In agreement with this result, the two conformers of n-propyl fluoride also have nearly the same internal rotation potential V_3. A comparison

Table 7. Internal rotation parameters of antiperiplanar butyronitrile. $w_1(s)$: first Fourier coefficient, I_α: moment of inertia of the methyl group, $\measuredangle(i, g)$: angle between the internal rotation axis i and the inertia axes g = a, b, s: reduced barrier height, F: reduced internal rotation constant, V_3: barrier height to internal rotation, σ: standard deviation of the fit. $\bar{\nu}$: mean experimental methyl torsion splitting. Assumed value in square brackets.

$w_1(s)$	$= -0.2334\,(26)\cdot 10^{-5}$		
I_α	$= 3.139\,(26)$ amu Å^2		
$\measuredangle(a,i)$	$= 20.39\,(88)^\circ$		
$\measuredangle(b,i)$	$= 69.61\,(88)^\circ$		
$[\measuredangle(c,i)$	$= 90.0^\circ]$		
F	$= 185.3\,(20)$ GHz		
s	$= 78.26\,(11)$		
V_3	$= 3.110\,(38)$ kcal/mol		
V_3	$= 13.02\,(16)$ kJ/mol		

$\sigma = 4$ kHz
$\bar{\nu} = 263$ kHz

Correlation coefficients matrix

$w_1(s)$	1.000		
I_α	−0.276	1.000	
$\measuredangle(a,i)$	−0.894	0.660	1.000

Table 8. Internal rotation parameters of synclinal butyronitrile. I_α: moment of inertia of the methyl group. $\measuredangle(i, g)$: angle between the internal rotation axis i and the inertia axes g = a, b, c. The other signs are used in the same way as in Table 7.

$w_1(s)$	$= -0.891\,(41)\cdot 10^{-6}$		
$[I_\alpha$	$= 3.139$ amu Å$^2]$		
$\measuredangle(a,i)$	$= 72.9\,(25)^\circ$		
$\measuredangle(b,i)$	$= 25.6\,(18)^\circ$		
$\measuredangle(c,i)$	$= 71.6\,(32)^\circ$		
F	$= 164.89\,(21)$ GHz		
s	$= 87.85\,(57)$		
V_3	$= 3.107\,(24)$ kcal/mol		
V_3	$= 13.01$ kJ/mol		

Correlation coefficient matrix

$w_1(s)$	1.000		
λ_+	0.711	1.000	
λ_-	−0.939	−0.891	1.000

$\lambda_+ = \cos^2\measuredangle(a,i) + \cos^2\measuredangle(b,i) = 1 - \cos^2\measuredangle(c,i)$
$\lambda_- = \cos^2\measuredangle(a,i) + \cos^2\measuredangle(b,i)$

$\sigma = 6$ kHz
$\bar{\nu} = 758$ kHz

Table 9. Internal rotation parameters of some propyl compounds $CH_3CH_2CH_2X$. Assumptions in square brackets, standard deviations in brackets.

	X = F (antiperipl.) [19]	X = F (syclinal) [19]	X = OH (trans) [20]
$w_1(s)$	$-0.7010\,(29)\cdot 10^{-5}$	$-0.2810\,(26)\cdot 10^{-5}$	–
I_α [amu Å^2]	3.157 (6)	3.168 (35)	[3.193]
$\measuredangle(a,i)$ [°]	26.71 (23)	55.54 (40)	29 (1)
$\measuredangle(b,i)$ [°]	63.29 (23)	38.74 (38)	61 (1)
$\measuredangle(c,i)$ [°]	[90.00]	74.49 (92)	[90.00]
F [GHz]	186.00 (48)	168.0 (19)	–
s	67.926 (33)	76.505 (95)	69.6 (15)
V_3 [kcal/mol]	2.7104 (84)	2.758 (35)	2.730 (60)

	X = CN (trans)	X = CN (gauche)	X = H [21]
$w_1(s)$	$-0.2334\,(26)\cdot 10^{-5}$	$-0.891\,(49)\cdot 10^{-6}$	$0.1909\,(29)\cdot 10^{-5}$
I_α [amu Å^2]	3.139 (26)	[3.139]	3.198 (21)
$\measuredangle(a,i)$ [°]	20.39 (88)	72.9 (25)	35.17 (64)
$\measuredangle(b,i)$ [°]	69.61 (88)	25.6 (18)	54.83 (64)
$\measuredangle(c,i)$ [°]	[90.00]	71.6 (32)	[90.00]
$\measuredangle(i,i)$ [°]	–	–	109.7 (12)
F [GHz]	185.3 (20)	164.89 (21)	183.99 (121)
s	78.26 (11)	87.85 (57)	80.22 (15)
V_3 [kcal/mol]	3.110 (38)	3.107 (24)	3.166 (27)

of n-propyl fluoride and butyronitrile shows that n-propyl fluoride has a distinctly lower barrier hight V_3. The corresponding V_3 potentials of the ethyl derivates are in inverse ratio to the potentials of the propyl compounds, namely ethyl fluoride: $V_3 = 3.349$ kcal/mol [17] and ethyl nitrile: $V_3 = 3.176$ kcal/mol [18].

We thank the members of our group for help and discussion, the Deutsche Forschungsgemeinschaft, the Land Schleswig-Holstein and the Fonds der Chemie for funds. The calculations were made at the computer center of the university.

[1] E. Hirota, J. Chem. Phys. **37,** 2918 (1962).
[2] V. K. Kaushik, Spectrochim. Acta **35a,** 851 (1979).
[3] J. Demaison and H. Dreizler, Z. Naturforsch. **37a,** 199 (1982).
[4] F. Nata and J. Perez, Spectrochim. Acta **40a,** 109 (1984).
[5] G. Wlodarczak, L. Martinache, J. Demaison, K.-M. Marstokk, and H. Møllendal, to be published.
[6] G. Bestmann, H. Dreizler, H. Mäder, and U. Andresen, Z. Naturforsch. **35a,** 392 (1980).
[7] G. Bestmann and H. Dreizler, Z. Naturforsch. **37a,** 58 (1982).
[8] W. Stahl, G. Bestmann, H. Dreizler, U. Andresen, and R. Schwarz, Rev. Sci. Instrum. **56,** 1759 (1985).
[9] W. Stahl, J. Gripp, N. Heineking, and H. Dreizler, Z. Naturforsch. **42a,** 392 (1987).
[10] I. Merke and H. Dreizler, Z. Naturforsch. **43a,** 196 (1988).
[11] J. Haekel and H. Mäder, Z. Naturforsch. **43a,** 203 (1988).
[12] J. K. G. Watson Aspects of Quartic and Sextic Centrifugal Effects on Rotational Energy Levels, in "Vibrational Spectra and Structure", J. R. Durig ed., Elsevier, New York 1977 p. 39.
[13] W. Gordy and R. L. Cook, Microwave Molecular Spectra, John Wiley, New York 1984, Chapt. IX, 4.
[14] R. C. Woods, J. Mol. Spectrosc. **21,** 4 (1966).
[15] R. C. Woods, J. Mol. Spectrosc. **22,** 49 (1967).
[16] Program KC3IAM author R. C. Woods modified by W. Kasten, Kiel.
[17] E. Fliege, H. Dreizler, D. Boucher, J. Burie, and A. Dubrulle, J. Chem. Phys. **78,** 3541 (1983).
[18] H. Mäder, H. M. Heise, and H. Dreizler, Z. Naturforsch. **29a,** 164 (1974).
[19] W. Kasten and H. Dreizler, Z. Naturforsch. **41a,** 955 (1986).
[20] H. Dreizler and F. Scappini, Z. Naturforsch. **36a,** 1126 (1981).
[21] G. Bestmann, W. Lalowski, and H. Dreizler, Z. Naturforsch. **40a,** 271 (1985).